Electronic Supplementary Material (ESI) for Environmental Science: Water Research & Technology.


# Dissolved oxygen and nitrate effects on the reduction and removal of divalent mercury by pumice supported nanoscale zero-valent iron

*Ghulam Hussain Qasim,[a] Sangwook Lee,[a] Giehyeon Lee,[b] Woojin Lee,[c] Yongseok Hong,[d] Seunghee Han[a]**

*[a]School of Earth Sciences and Engineering, Gwangju Institute of Science and Technology (GIST), Gwangju 61005, Republic of Korea*

*[b]Department of Earth System Sciences, Yonsei University, Seoul 120-749, Republic of Korea*

*[c]Department of Civil and Environmental Engineering, Green Environmental and Energy Lab., National Laboratory Astana, Nazarbayev University, Astana 010000, Republic of Kazakhstan*

*[d]Department of Environmental Systems Engineering, Korea University, Sejong City 30019, Republic of Korea*

*Corresponding author

phone: 82-62-715-2438, fax: 82-62-715-2434, e-mail: shan@gist.ac.kr

**Tables S1-S4, Figures S1-S11**

**Table S1** X-ray fluorescence (XRF) data for chemical composition of pumice.

| | Compound name | Concentration (%) |
|---|---|---|
| 1 | $SiO_2$ | 70.77 |
| 2 | $Al_2O_3$ | 14.01 |
| 3 | $Na_2O$ | 4.68 |
| 4 | $Fe_2O_3$ | 3.19 |
| 5 | CaO | 3.14 |
| 6 | $K_2O$ | 2.06 |
| 7 | MgO | 1.26 |
| 8 | $TiO_2$ | 0.38 |
| 9 | $SO_3$ | 0.16 |

**Table S2** Change in surface area of pumice, nZVI, and p-nZVI before and after reaction with Hg.

| | | Conditions | BET Surface Area ($m^2$ $g^{-1}$) |
|---|---|---|---|
| Before Reaction | Pumice | - | 0.43 |
| | nZVI | - | 18.3 |
| | p-nZVI | - | 0.83 |
| After Reaction | p-nZVI | Oxic | 20.3 |
| | | Anoxic | 10.3 |
| | PnZVI + Nitrate (mM) | Oxic | 13 |
| | | Anoxic | 7.7 |

**Table S3** Comparison between Langergren pseudo first order and pseudo second order (type 1) kinetic models for Hg adsorption by p-nZVI. Hg concentration was 250 nM and p-nZVI concentration with 7.7% iron fraction was added as 0.364, 3.64 and 36.4 g $L^{-1}$. Experimental $q_e$ was 1219, 139, and 15.5 for pumice 0.364, 3.64, and 36.4 g $L^{-1}$, respectively. The $q_e$ is a model value of the mass of Hg adsorbed (mg $g^{-1}$), $K_{1,m}$ ($min^{-1}$) and $K_{2,m}$ (g $\mu g^{-1}$ $min^{-1}$) are pseudo first and pseudo second order sorption rate constants. The $K_{1,sa}$ (g $min^{-1}$ $m^{-2}$) and $K_{2,sa}$ ($g^2$ $\mu g^{-1}$ $min^{-1}$ $m^2$) are surface area normalized pseudo first and pseudo second order sorption rate constants.

| | p-nZVI 0.364 g $L^{-1}$ | | | | p-nZVI 3.64 g $L^{-1}$ | | | | p-nZVI 36.4 g $L^{-1}$ | | | |
|---|---|---|---|---|---|---|---|---|---|---|---|---|
| Pseudo 1st order | $q_e$ | $k$ | $k_{sa}$ | $r^2$ | $q_e$ | $k$ | $k_{sa}$ | $r^2$ | $q_e$ | $k$ | $k_{sa}$ | $r^2$ |
| | $\mu g\ g^{-1}$ | $min^{-1}$ | g $min^{-1}$ $m^{-2}$ | | $\mu g\ g^{-1}$ | $min^{-1}$ | g $min^{-1}$ $m^{-2}$ | | $\mu g\ g^{-1}$ | $min^{-1}$ | g $min^{-1}$ $m^{-2}$ | |
| | 1121 | 0.0245 | 0.0295 | 0.988 | 66.4 | 0.0177 | 0.0213 | 0.800 | 6.8 | 0.0179 | 0.0216 | 0.780 |
| Pseudo 2nd order | $\mu g\ g^{-1}$ | g $\mu g^{-1}$ min-1 | $g^2$ $\mu g^{-1}$ $min^{-1}$ $m^2$ | | $\mu g\ g^{-1}$ | g $\mu g^{-1}$ $min^{-1}$ | $g^2$ $\mu g^{-1}$ $min^{-1}$ $m^2$ | | $\mu g\ g^{-1}$ | g $\mu g^{-1}$ $min^{-1}$ | $g^2$ $\mu g^{-1}$ $min^{-1}$ $m^2$ | |
| | 1308 | 0.0002 | 0.0002 | 0.999 | 142.2 | 0.0047 | 0.0057 | 0.999 | 15.8 | 0.0585 | 0.0705 | 0.999 |

**Table S4** The peak area ratio of Fe(0), Fe(II) and Fe(III) in Figures 2 and S10, and that of Hg(0) and Hg(II) in Figure 4.

| Sample ID | Fe(0) | Fe(II) | Fe(III) | Hg(II) | Hg(0) |
|---|---|---|---|---|---|
| nZVI before reaction | 12.4 | 7.0 | 80.6 | N/D | N/D |
| After oxic reaction | 0.0 | 0.0 | 100.0 | 92.5 | 7.5 |
| After anoxic reaction | 10.3 | 8.9 | 80.8 | 84.7 | 15.3 |
| $NO_3$-after oxic reaction | 0.0 | 1.7 | 98.3 | N/D | N/D |
| $NO_3$-after anoxic reaction | 0.0 | 1.9 | 98.1 | N/D | N/D |

**Figure S1** Morphology of p-nZVI: SEM image of (a) p-nZVI with 1.93% Fe mass fraction, (b) p-nZVI with 3.85% Fe mass fraction, (c) p-nZVI with 7.7% Fe mass fraction, and (d) bare pumice.

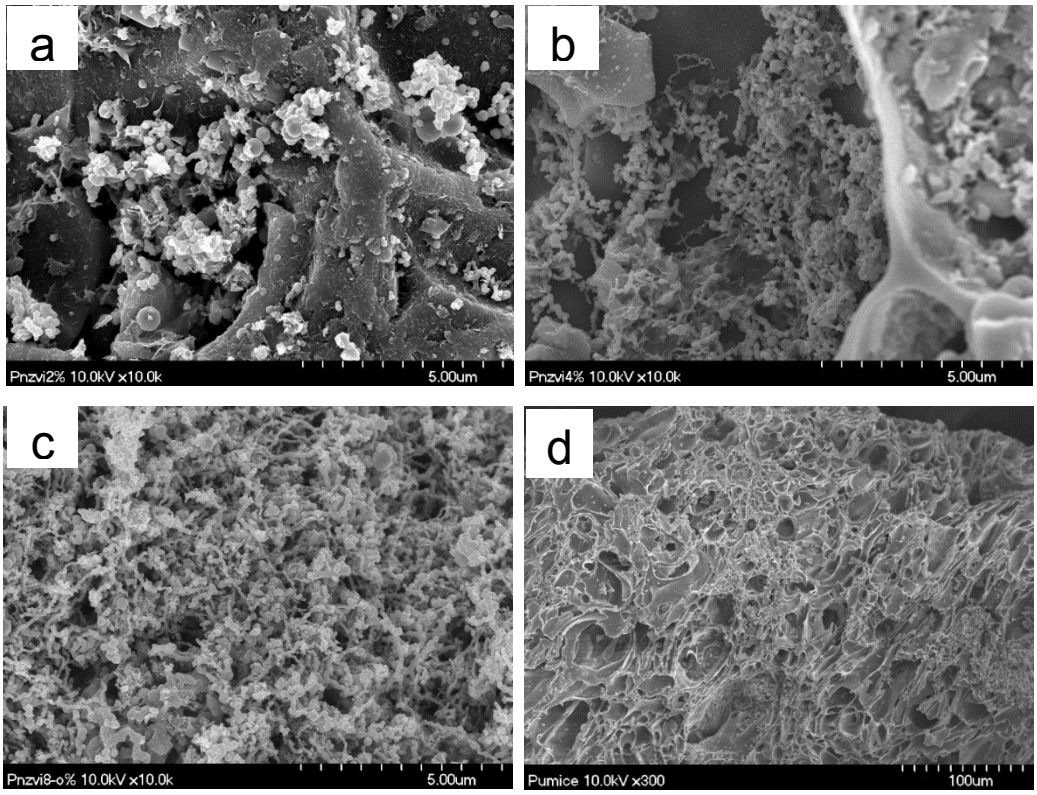

**Figure S2 (a)** Morphology of p-nZVI with 7.7% Fe fraction, and (b) Energy Dispersive Spectroscopy (EDS) data of p-nZVI with 7.7% Fe fraction.

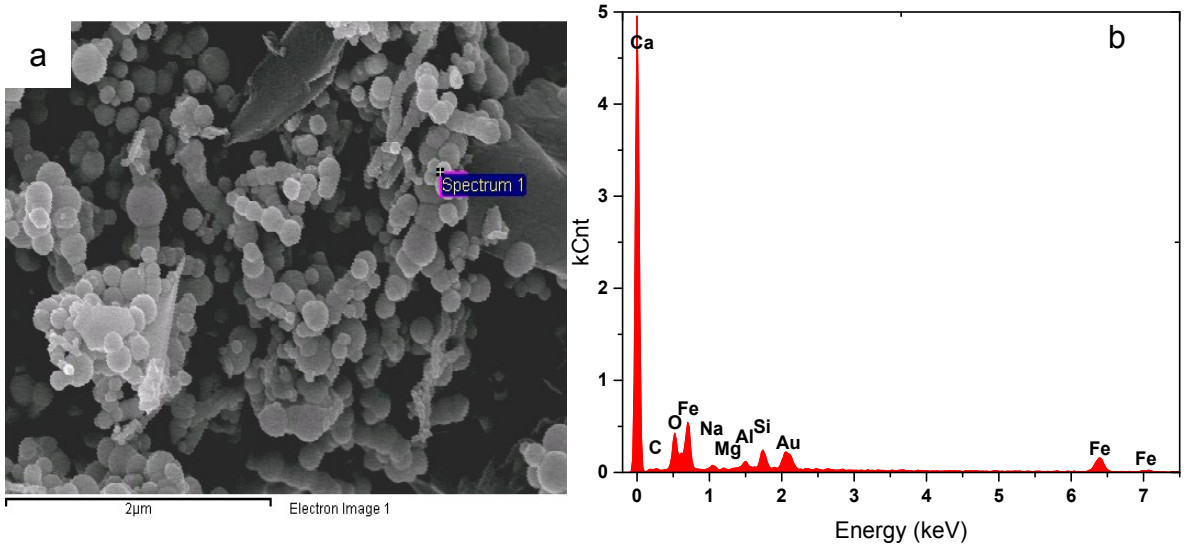

**Figure S3** (a) Effects of p-nZVI loading on the aqueous Hg(II) removal, (b) sorption rate constant calculated by pseudo second order kinetic model versus Fe loading, (c) Hg removal and reduction by pumice without nZVI, and (d) Hg(II) reduction by nZVI and p-nZVI. In (a) and (b) Hg(II) concentration was 250 nM, p-nZVI loading was 0.364, 3.64 and 36.4 g $L^{-1}$ and pumice loading was 36.4 g $L^{-1}$ in HEPES buffer solution of pH 7. In (c) Hg(II) concentration was 250 nM and pumice loading was 36.4 g $L^{-1}$ in HEPES buffer solution of pH 7. In (d) Hg(II) concentration was 250 nM, nZVI loading was 0.28 g $L^{-1}$, and p-nZVI loading was 3.64 g $L^{-1}$ in HEPES buffer solution of pH 7.

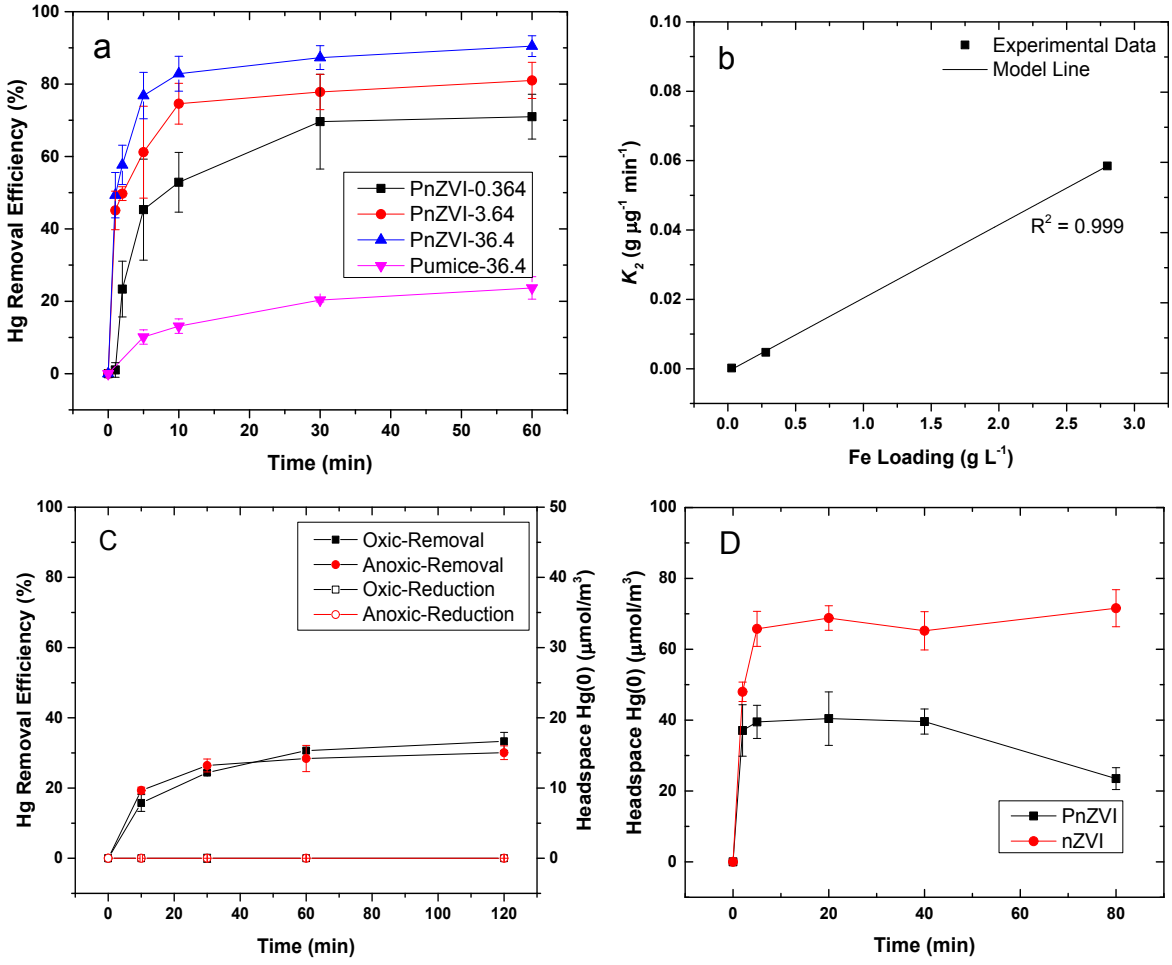

**Figure S4** Effect of Hg loading (25, 250, 1000, and 2500 nM) on (a) Hg(II) removal and (b) Fe(II) dissolution. The final p-nZVI concentration in HEPES buffer solution of pH 7 was 36.4 g $L^{-1}$. Fe(II) and Hg concentrations were determined after 2 hours of reaction.

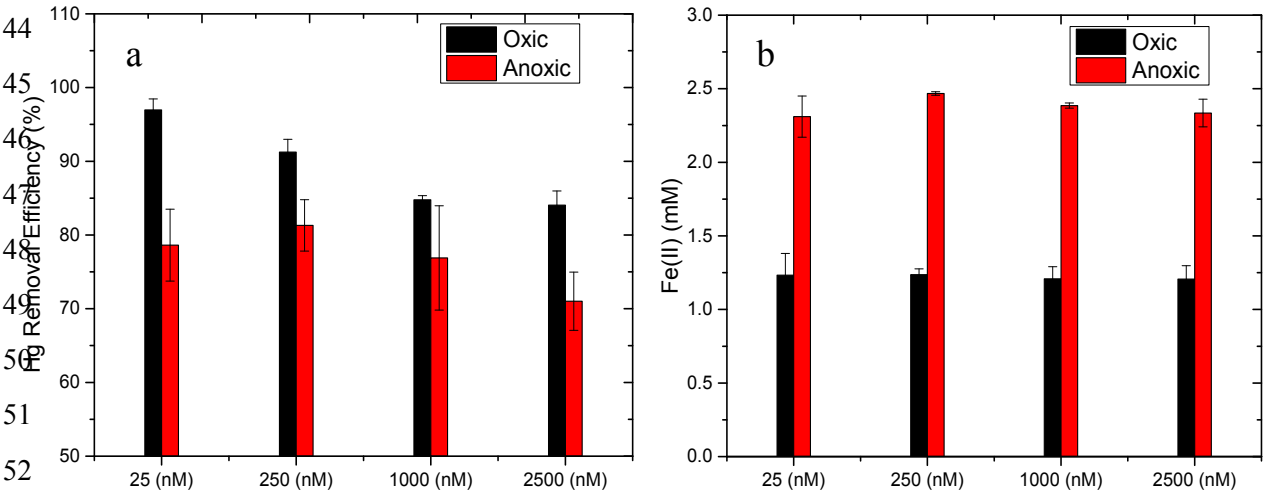

**Figure S5** Pictures of reaction vials in (a) oxic and (b) anoxic conditions before and after two hours of Hg(II) reaction. Initial Hg(II) concentration was 250 nM and p-nZVI was 36.4 g $L^{-1}$ in HEPES buffer solution of pH 7.

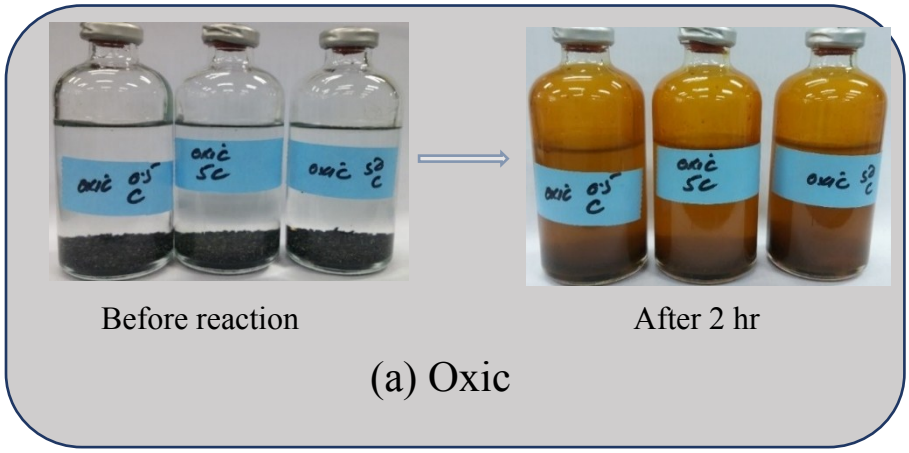


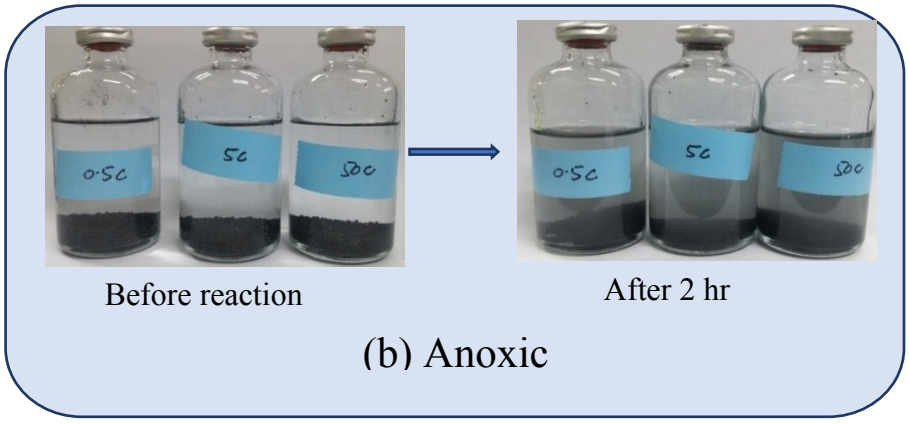

**Figure S6** X-ray diffraction (XRD) analysis of secondary iron minerals of nZVI reacted with Hg in oxic and anoxic conditions with and without nitrate. Initial Hg(II) concentration was 5 mM, nZVI was 11.2 g $L^{-1}$ and nitrate was 32 mM in HEPES buffer solution of pH 7.

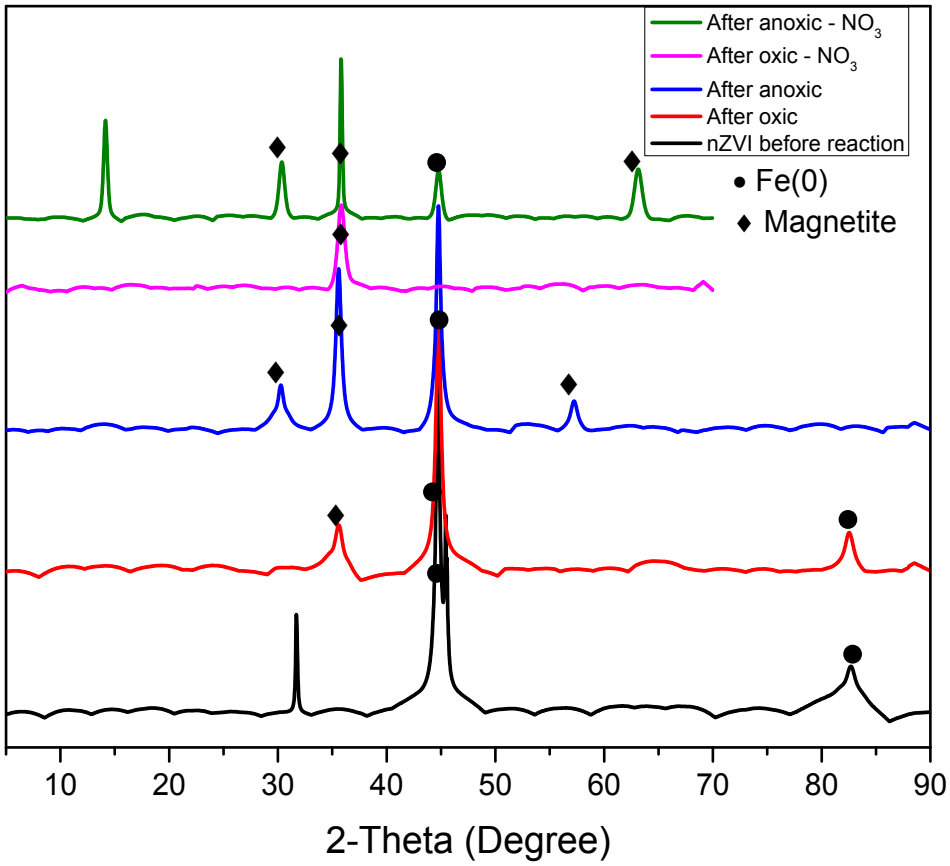

**Figure S7** TEM images of nZVI: (a) before reaction with Hg(II), (b) after reaction with Hg(II) in oxic condition, (c) after reaction with Hg(II) in anoxic condition, (d) after reaction with Hg(II) in oxic condition with 8 mM of nitrate, and (e) after reaction with Hg(II) in anoxic condition with 8 mM of nitrate. Initial Hg(II) concentration was 250 nM and p-nZVI was 36.4 g $L^{-1}$ in HEPES buffer solution of pH 7.

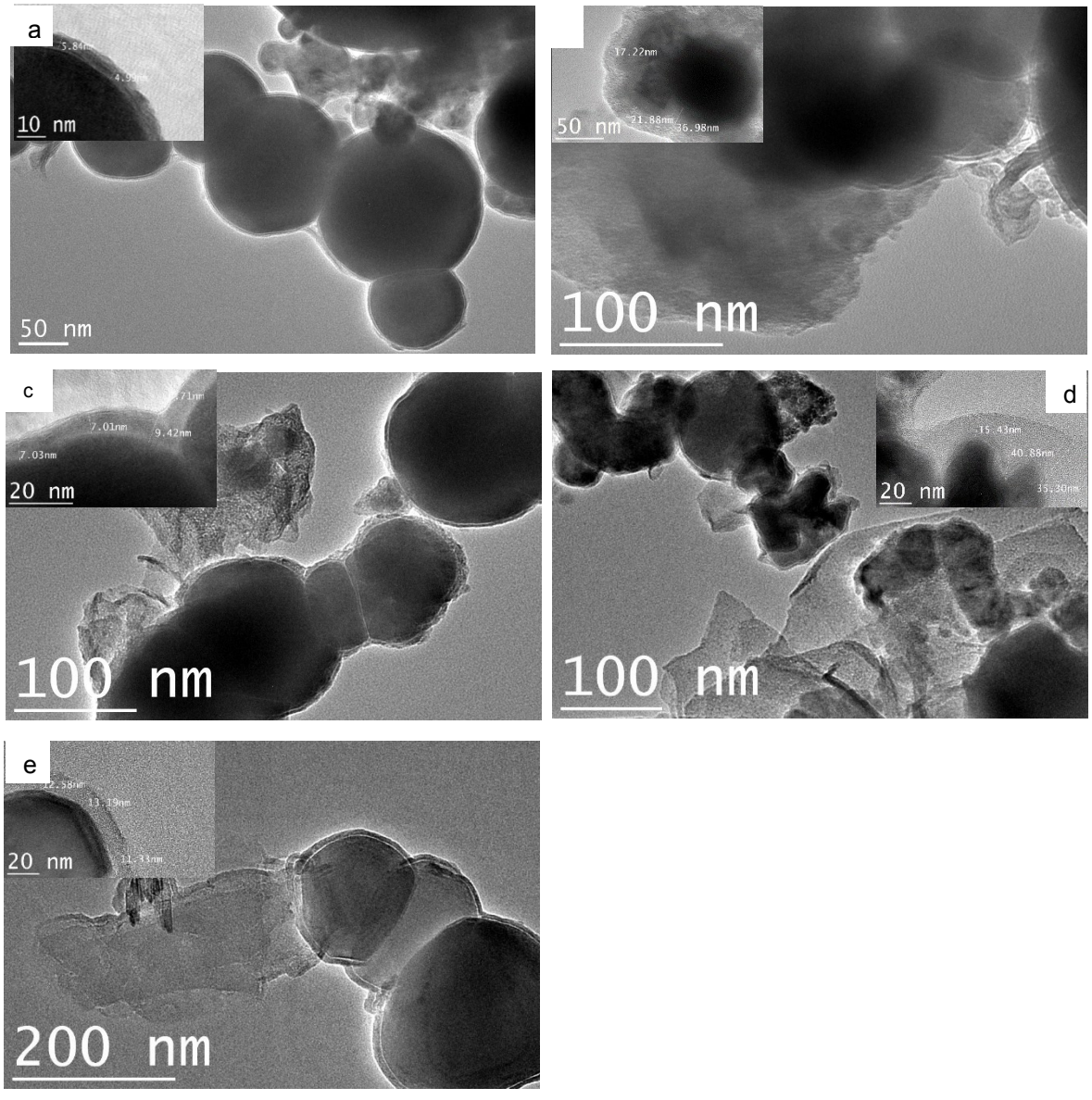

**Figure S8** Increase of headspace Hg(0) in the presence of aqueous Fe(II) as $FeCl_2$ under oxic condition. Initial Hg(II) was 1500 nM, and $FeCl_2$ was 44 and 57 mM in HEPES buffer solution of pH 7.

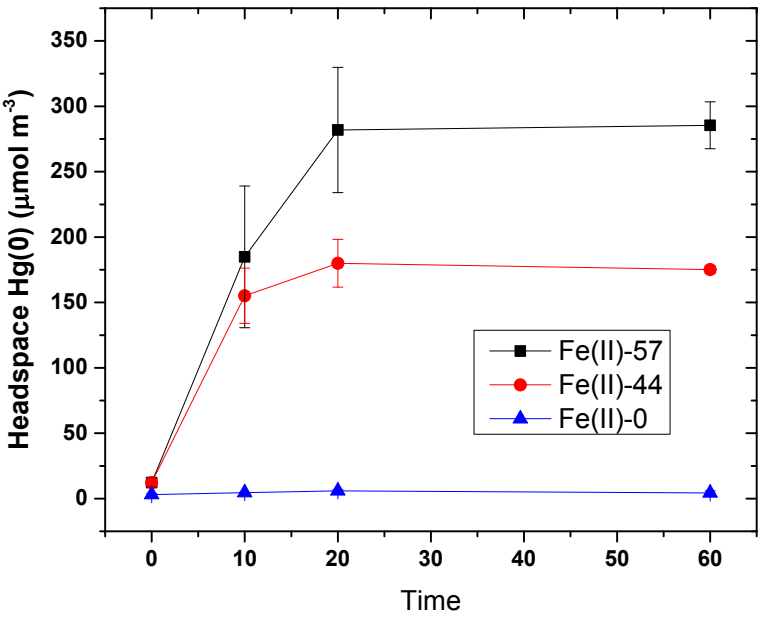

**Figure S9** Decrease of headspace Hg(0) in the presence of amorphous FeO(OH) in oxic and anoxic conditions. Initial Hg(0) in headspace was 10 μmol $m^{-3}$ and FeO(OH) in solution was 4.4 g $L^{-1}$ in HEPES buffer solution of pH 7.

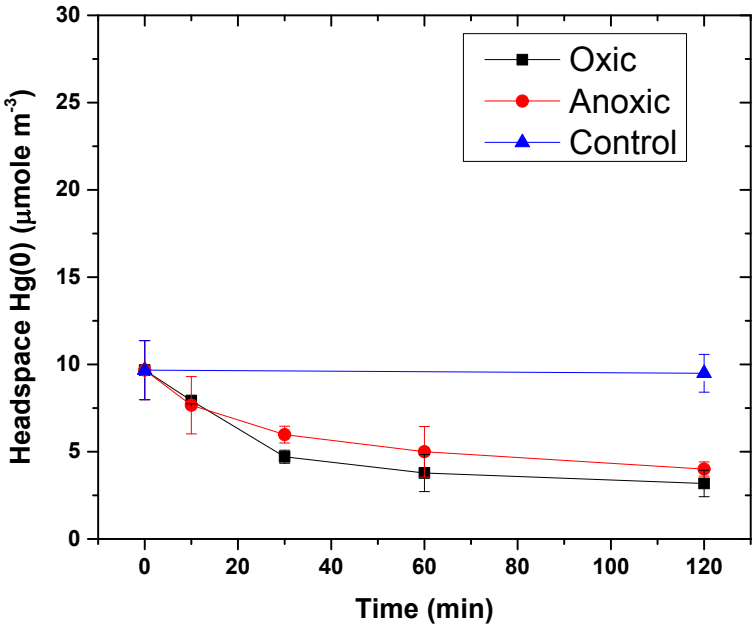

**Figure S10** Changes of nitrate and ammonium concentrations after reaction with p-nZVI in the presence of Hg(II) in (a) oxic and (b) anoxic conditions. Initial nitrate concentration was 8 mM, Hg(II) was 250 nM, and p-nZVI was 36.4 g $L^{-1}$ in HEPES buffer solution of pH 7.

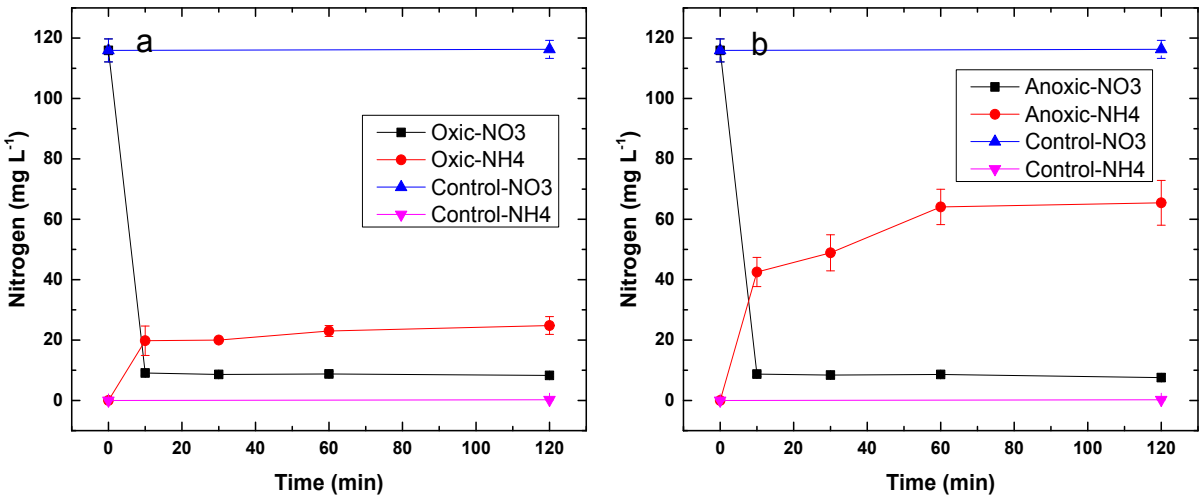

**Figure S11** High resolution XPS spectra of Fe2p3 in nZVI after reaction with nitrate and Hg. Initial Hg(II) concentration was 5 mM, nZVI was 11.2 g $L^{-1}$ and nitrate was 32 mM in HEPES buffer solution of pH 7.